



Welsby, H. J., & Hendry, K. R. (2016). The role of benthic biofilm production in the mediation of silicon cycling in the Severn Estuary, UK. *Estuarine, Coastal and Shelf Science*, 176, 124-134.
<https://doi.org/10.1016/j.ecss.2016.04.008>

Peer reviewed version

License (if available):
CC BY-NC-ND

Link to published version (if available):
[10.1016/j.ecss.2016.04.008](https://doi.org/10.1016/j.ecss.2016.04.008)

[Link to publication record in Explore Bristol Research](#)
PDF-document

This is the author accepted manuscript (AAM). The final published version (version of record) is available online via Elsevier at 10.1016/j.ecss.2016.04.008. Please refer to any applicable terms of use of the publisher.

University of Bristol - Explore Bristol Research

General rights

This document is made available in accordance with publisher policies. Please cite only the published version using the reference above. Full terms of use are available:
<http://www.bristol.ac.uk/red/research-policy/pure/user-guides/ebr-terms/>

The role of benthic biofilm production in the mediation of silicon cycling in the Severn Estuary, UK

Welsby, H.J.^{1,2}, Hendry, K.R.², Perkins, R.G.¹

¹School of Earth and Ocean Science, Main Building, Cardiff University, Cardiff, CF10 3AT, UK.

²School of Earth Sciences, University of Bristol, Wills Memorial Building, Queens Road, Bristol, BS8 1RJ, UK.

Abstract

The biological mediation of benthic biogenic silica (BBSi) by the diatom-dominated biofilms on the intertidal mudflats of the Severn Estuary (UK) was assessed *in situ* under different environmental conditions using measurements of productive biomass (chlorophyll *a*), photosynthetic activity of undisturbed microalgal assemblages, benthic biogenic silica (BBSi) and benthic dissolved silica (BDSi). We show low BBSi standing stocks in the mudflats compared to other European estuaries, under both warmer summer conditions (0.6%) and colder winter conditions (0.5%). Dissolved forms of Si (BDSi) dominated the estuary, with significantly higher concentrations during the sampled winter ($22.6 \pm 1.0 \text{ mg L}^{-1}$) compared to the sampled summer ($2.9 \pm 0.5 \text{ mg L}^{-1}$). Benthic algal biomass was higher under cold conditions compared to warmer conditions (24.0 ± 2.3 and $13.2 \pm 1.9 \text{ mg g}^{-1} \text{ sed. dw.}$, respectively), following reduced migratory behaviour in the winter increasing surficial biomass. Relative maximum Electron Transport Rate (rETR_{max}), used as a proxy for relative primary productivity, was higher under warm conditions ($254.1 \pm 20.1 \text{ rel. units}$) compared to cold conditions ($116.0 \pm 27.1 \text{ rel. units}$). The biofilms sampled in the summer biologically mediated Si by the productive, high light acclimated diatoms that were highly motile during fluorescence measurements, and exhibited migratory behaviour, which despite nutrient limitation, evidenced by low F_v/F_m , increased the accumulation of BBSi. The biofilms sampled in the winter that were subject to relatively colder temperatures, consisted of low light acclimated diatoms of reduced migratory capabilities, and induced NPQ that suppressed productivity, and mediated BBSi to a lesser extent. Environmental stresses reduced biofilm mediation of Si, which, in addition to high

hydrodynamic energy increasing biofilm re-suspension, controlled Si to a lesser extent compared to terrestrial/coastal inputs.

Keywords

Biogenic silica, benthic, biomass, primary productivity, downregulation.

Introduction

Most research on the global silicon (Si) cycle has focused on weathering (Hurd, 1977; West et al. 2005; Fortner et al. 2012) or oceanic Si cycles (Brzezinski et al. 1998; Yool & Tyrrell, 2003). Few have explored the complexity of the marine-terrestrial interconnecting cycles, leaving estuarine processes poorly constrained despite their importance in determining marine Si budgets. The present study intends to address the lack of research on Si cycling in the coastal transition zone. This was achieved by analysing the variations in Si fractions in the Severn Estuary, resulting from environmental driven changes in the ecosystem functioning, in the form of biomass and relative primary productivity, by the exposed diatom-dominated (Underwood, 2010) microphytobenthos (MPB) biofilms on the intertidal mudflats.

The high water turbidity, typical of a sediment-dominated estuary, limits the growth of large pelagic phytoplankton communities (Underwood, 2010). Subsequently, the MPB biofilms have high rates of biogeochemical cycling, with complex rhythms of photosynthetic activity (Pickney & Zingmark, 1991), and are likely to mediate nutrient dynamics in an estuary. MPB are characterized by the absence of photo-inhibition at high irradiance, due to the combination of physiological (e.g. effective photochemical and non-photochemical quenching, NPQ; see Maxwell & Johnson, 2000; Jesus et al. 2006; Lavaud & Kroth, 2006) and behavioural mechanisms (bulk migratory response), and cell surface turnover in the form of micro-cycling, minimizing the risk of overexposure to damaging light intensities (Kromkamp et al. 1998; Serôdio et al. 2006b, 2008; Perkins et al. 2001, 2002, 2010). No previously published studies have investigated the diatom-dominated MPB biofilms influence on Si dynamics in the Severn Estuary.

The Severn Estuary is a heterogeneous environment with a complex hydro-geomorphology (Kirby, 2010; Manning et al. 2010), resulting in an important environment for biosphere functioning, primarily through the filter for land-ocean exchange. The hyper-tidal range is the second highest astronomical tide globally (13.9

m at Avonmouth) (Liang et al. 2013) resulting in substantial intertidal areas of cohesive muddy sediment. This makes the Severn Estuary an important case study for Si cycling, and allows for scaling to quantify other estuarine Si budgets. Few estuarine Si studies exist globally (De'Elia et al. 1983; Rendell et al. 1997; Liu et al. 2005; 2008; 2009; Arndt & Regnier, 2007; Pastuszak et al 2008; Carbonnel et al. 2009; 2013), and understanding of the controls on the current Si cycle and estuarine budgets are lacking. The Scheldt Estuary, Belgium/The Netherlands, remains one of the only estuaries to have a comprehensive Si dataset, and has proven to enhance biological processes leading to nutrient transformations (Arndt & Regnier, 2007; Carbonnel et al. 2009; 2013). Similarly, the fine-sediment dominated Severn Estuary may exhibit a significant biological control on Si dynamics. Further, the strength of the inter-habitat coupling in the estuary implies that changes in MPB biomass and productivity may propagate into other linked ecosystems, and further afield to the marine pelagic zone in the southwest.

Si is a key element for siliceous organisms in aquatic habitats. Land-sea interactions and transfers control the proportions of Si in the form of silicic acid $\text{Si}(\text{OH})_4$, hereafter called 'dissolved silica' (DSi), and particulate biogenic silica (BSi). These vary seasonally and geographically due to the transformation from DSi to BSi ($\sim 240 \text{ t mol y}^{-1}$) by photoautotrophic motile epipellic diatoms (accounting for >95% of eukaryotic living cells on intertidal mudflats) (Underwood, 2010), and weathering processes, a factor of river flow regime and temperature (Ragueneau et al. 2000). The variation in the natural abundance of Si fractions has often been used as a proxy for diatom production and Si utilization (Conley & Malone, 1992). Therefore, characterizing the difference in Si fractions provides important information on Si biological uptake in the estuary.

Si cycling is poorly quantified from local to global scales due to the lack of Si data compared to other key nutrients (Moosdorf et al. 2011). Previous studies (Conley & Malone, 1992; Aure et al. 1998; Gilpin et al. 2004) have noted non-Redfield ratios (Redfield et al. 1963) in estuaries. For example, in sub areas of the Baltic Sea, the doubling of phosphate and nitrate inputs increased BSi production causing a reduction in DSi, and induced Si limitation (Pastuszak et al. 2008). Such nutrient ratios can diminish the relative importance of diatoms, resulting in non-siliceous phytoplankton becoming dominant (Correll et al. 2000). Despite the Severn Estuary's ecological and economic importance, its role in benthic BSi (BBSi) and benthic DSi (BDSi) transformations, to our knowledge, has not been addressed quantitatively. This gap

leaves little understanding of the terrestrial disturbances by anthropogenic activities, land-use changes, and climate change expected over the twenty-first century (Met Office, 2011). The aim of this study was to analyse the biological mediation of Si by the diatom-dominated MPB biofilms in the Severn Estuary under different environmental conditions, resulting from investigating three separate survey sites under summer and winter conditions. This was achieved through the analysis of different environmental conditions experienced during the summer (relatively warmer, lower rainfall) and a winter (relatively colder, higher rainfall), and over a spatial scale of the three sample sites that differed in sediment water content and site exposure.

Methods

Study site and sampling method

The study was carried out on intertidal mudflats located in the Severn Estuary between southeast Wales and southwest England (Fig. 1). Three intertidal mudflat sites were surveyed: site 1, Severn Beach (002°66'W, 051°56'N); site 2, Portishead (002°77'W, 051°49'N); and site 3, Newport Wetlands (002 °58'W, 051°32'N). Site 1 mudflats located at the mouth of the River Severn, subject to a small tidal prism, were exposed to the full-force of the prevailing south westerly winds, and had sediments of high sand content (>63 µm). Site 2 mudflats were less exposed to the south westerly winds, and had higher mud content (<63 µm), and crevasses perpendicular to the shoreline. Site 3 mudflats, subject to a large tidal prism, were sheltered from the south westerly winds, and had high mud content (<63 µm), and laid adjacent to a saltmarsh and wetlands.

In situ MPB biofilms were sampled during daytime low tide periods in the summer and winter of 2014. Air temperature records for the Severn Estuary show a significant difference ($t(df)=13.224$, $p<0.001$) between the relatively warmer summer and relatively colder winter sampling periods (Fig. 2) (Met Office, 2015). The benthic biofilms sampled during the summer were exposed to longer sunshine hours and lower rainfall (225 hrs sunshine, 79.6 ± 28.2 mm of rain) compared to biofilms sampled during the winter (64 hrs sunshine and 136.8 ± 28.6 mm of rain) (Met Office, 2015).

At each site, 12 sampling stations were surveyed, equally spaced along a linear transect parallel to the lower shore. Sampling involved extracting sediment mini-cores of a diameter of 2.54 cm for the surficial 5 mm biofilm for analyses of chlorophyll *a* content (chl *a*) (Smith & Underwood, 1998), key benthic diatom species, and BBSi

content. Pore fluids (25 ml) at each station were sampled for BDSi and orthophosphate (P) concentrations using a simplified peeper method (Teasdale et al. 1995).

BBSi

Approximately 25% of the surficial 5 mm biofilm sediment was placed in an oven at 85°C for 24 h to determine the percentage loss of weight upon drying. BBSi concentrations were determined following the standard alkaline extraction method for marine sediment (DeMaster, 1981) and presented as percentage of dried Si mass (g/g). Dried sediment was crushed using a pestle and mortar, and ~0.05 g of the sediment was leached in hydrogen peroxide (5 ml of 10% H₂O₂ solution), followed by acid (5 ml of 1M HCl solution). To each sample, 40 ml of 0.1 M of NaCO₃ was added. Samples were placed in a covered, constant temperature water bath at 85°C. After 1 h, 3 h and 5 h, sub samples were taken, diluted, neutralized, and analysed for BBSi content using the standard Heteropoly Blue Method, and measured using a Hach Lange DR3900 spectrophotometer.

BDSi and orthophosphate (P-PO₄⁻)

Pore fluid samples were centrifuged for 10 min at 1000 rpm for BDSi and P-PO₄⁻ concentrations. BDSi was analysed using the Heteropoly Blue method with concentrations (mg L⁻¹) measured using a Hach Lange DR3900 spectrophotometer. P-PO₄⁻ concentrations (mg L⁻¹) from pore fluids were measured using a Hach Lange DR3900 spectrophotometer, where 2.0 ml of each sample were analysed following the LCK 349 method. All P-PO₄⁻ concentrations recorded in both seasons, were below 50 mg L⁻¹ and did not interfere with BBSi measurements.

MPB biofilm biomass and key species

Half of the surficial 5 mm of the sediment from the mini-cores was extracted, weighed (g) and corrected for water content (loss of weight upon drying at 85°C for 24 h) (see Perkins et al. 2003). Productive biomass via chl *a* content (mg g⁻¹ *sed. dw.*) were determined following the standard method (extraction in methanol; Schwartz & Lorenzo, 1990), with 4 ml of methanol buffered with MgCO₃ added to each sediment sample and left at -4°C and in the dark for 24 h. Samples were vortex mixed and centrifuged at 2000 rpm for 15 min. Chl *a* values were corrected for phaeopigments through acidification following the standard method (Lorenzen, 1966), with absorbance measured at 665 nm and 750 nm and repeated following the addition of 1 drop of 10% HCl to each plastic micro-cuvette.

Species composition of the biofilms were determined by filtering approximately 25% of

the surficial 5 mm sediments with DI water to remove silts and fine sediment grains. Due to the low biomass, the suspended fractions were placed in petri dishes and diatoms were viewed using bright-field microscopy for the determination of key diatoms species. Individual diatoms were mounted, dried and gold plated for imaging using the Environmental Scanning Electron Microscope (FEI XL30 ESEM FEG).

Chlorophyll fluorescence

Variable chlorophyll fluorescence of undisturbed microalgae assemblages was determined using a Water Pulse Amplitude Modulated (PAM) fluorometer equipped with an EDF/B fibre optic detector (blue light measuring beam and actinic light). The Water PAM 6 mm diameter Fluid Light Guide fiberoptics probe bundle (that delivered the measuring and saturating light provided by the fluorometer) was applied to the surface of the mudflat perpendicularly, at a fixed distance of 2 mm and an area of 0.28 cm². A low frequency, non-actinic measuring beam and a 0.6 s saturation pulse of ~8000 $\mu\text{mol m}^{-2} \text{s}^{-1}$ photosynthetically available radiation (PAR) were used (see Table 1 for notation). The fluorometer photomultiplier signal gain was set at a level to ensure fluorescence yields of >300 units for all measurements (with a new auto zero set each time the gain was altered). The external irradiance levels were logged at each station using the PAM light sensor. All data were stored and downloaded using WinControl-3 software.

The saturating pulse was applied to the sediments and the operational photosystem II chl fluorescence yield in actinic light (F') was recorded. The fluorescent parameter F_m (in the dark, first step of a rapid light curve) and F_m' (in the light, subsequent steps of a rapid light curve), the maximum PSII chl fluorescence yield in actinic light when all reaction centres are closed, are often underestimated (see Serôdio et al. 2005) due to retained non-photochemical down regulation in the dark (Perkins et al. 2010). Therefore, the maximum F_m' value ($F_{m' \max}$), higher than F_m , measured under low actinic light, is used for the calculation of associated photophysiological parameters (e.g. NPQ, F_v/F_m , see *below*). The maximum quantum efficiency of PSII (F_q'/F_m') was calculated as $(F_m' - F')/F_m'$. Rapid Light Curves (RLCs) were produced following Perkins et al. (2006) for the determination of the maximum relative Electron Transport Rate ($rETR_{\max}$), light saturation coefficient (E_k) and the light use coefficient for PSII (α), derived from curve fitting the model of Eilers & Peeters (1988) using Sigmaplot curve fitter (Systat Software Inc., San Jose). RLCs consisted of the fluorescence responses to nine different actinic irradiances of 20 s duration. The model consisted of an iterative solution to the curve with 100 iterations processed and significant ($p < 0.001$)

coefficients of a , b and c (Eilers & Peeters, 1988). Some individual RLCs saturated, with these coefficients used to calculate $rETR_{max}$ and α . However, some RLCs failed to saturate, therefore $rETR_{max}$ and E_k could not be calculated. $rETR_{max}$ was hence estimated as the highest value at the end of the RLC and is used here as a proxy for relative primary productivity. α was also calculated as the initial slope of the RLC simply from:-

$\alpha = (\Delta rETR / \Delta PAR)$ over the first two light curve steps.

The maximum quantum yield of PSII in the dark-adapted state, used as a proxy for MPB biofilm health/nutrient limitation, F_v/F_m (Genty et al., 1989) was calculated as:-

$$F_v/F_m = (F_m'_{max} - F_o)/F_m'_{max}$$

The fluorescent parameters of $F_m'_{max}$ and F_m' were used to calculate downregulation of photochemistry (Lavaud, 2007), in the form of non-photochemical quenching (NPQ):-

$$NPQ = ((F_m'_{max} - F_m')/F_m').$$

Maximum NPQ (NPQ_{max}) was estimated from each light curve based upon the peak NPQ value. Proportional changes of F' and F_m' were analysed to determine whether diatoms were vertically migrating or undergoing NPQ reversal/induction (see Perkins et al. 2010).

Statistical analysis

To determine the variability in biofilm mediation of Si between warm and cold periods, the existence of significant difference ($p < 0.001$) between summer and winter sampled periods was tested. Data (BBSi, BDSi, P-PO₄⁻, chl *a* and water content) which failed normal distribution (Kolmogorov Smirnov test) and homogeneity of variance (Levene's test) was tested using Mann-Whitney U. Data ($rETR_{max}$ and irradiance levels) which had normal distribution (Kolmogorov Smirnov test) and homogeneity of variance (Levene's test) was tested using a Two-tailed Student's t-test. The significant ($p < 0.05$) variability between sites within each season was tested using a Kruskal-Wallis test and one-way ANOVA. The relationship between biological variables and Si was tested, with linear relationships assessed using Pearson's correlations.

Results

BBSi and BDSi intertidal mudflat standing stocks

The Severn Estuary intertidal mudflats had low standing stocks of particulate Si in the form of BBSi during the summer (0.6%) and winter (0.5%) sampled periods of 2014 (Fig. 2), compared to previous benthic Si estuarine studies (e.g. Chou & Wollast, 2006; Arndt & Regnier, 2007). BBSi was significantly higher ($U_{df}=362.5$, $Z=-3.2118$, $p < 0.001$)

under warm conditions compared to cold conditions. BBSi standing stocks were significantly higher during the sampled summer ($H_{(2)}=16.31$, $p<0.05$) and winter ($H_{(2)}=23.2$, $p<0.05$) periods at site 3, nearest to the marine zone, compared to other sampled sites. As a result of local sediment conditions, BBSi varied spatially between the sampled sites, with lower BBSi concentrations at sites 1 (high sand content) compared to high concentrations at site 3 (high mud content), under both warm and cold conditions (Fig. 3). Water content was significantly lower during the warm ($H_{(2)}=27.73$, $p<0.001$) and cold ($H_{(2)}=15.07$, $p<0.001$) periods at Site 1 (exposed and high sand content), compared to site 3 (sheltered and high mud content).

Si in the Severn Estuary was predominantly present in dissolved forms (Fig. 2). BDSi concentrations in the mudflats were significantly greater ($U_{df=1}$, $Z=-7.2815$, $p<0.001$) under relatively colder conditions ($22.6 \pm 1.0 \text{ mg L}^{-1}$) compared to relatively warm conditions ($2.9 \pm 0.5 \text{ mg L}^{-1}$) (Fig. 2). Standing stocks of BDSi was greater at site 3 during the warmer summer, with concentrations averaging $4.2 \pm 1.2 \text{ mg L}^{-1}$ compared to site 1 and 2 (av. $2.2 \pm 0.4 \text{ mg L}^{-1}$). Under these warm conditions at site 1, chl a positively correlated with BDSi (Table 3). The highest standing stock of BDSi was recorded at site 1 during the colder winter period, near the mouth of the River Severn, with concentrations averaging $24.7 \pm 1.6 \text{ mg L}^{-1}$, potentially resulting from increased river flow following high rainfall (Fig.2). Furthermore, BDSi positively correlated with chl a during the winter sampled period (Table 3).

P- PO_4^- concentrations were greatest during the relatively colder winter period ($0.18 \pm 0.02 \text{ mg L}^{-1}$) compared to the warm summer period ($0.16 \pm 0.02 \text{ mg L}^{-1}$) (Fig. 3), but lacked significant variation. P- PO_4^- sampled in the summer negatively correlated with BBSi (Table 3). Furthermore, P- PO_4^- concentrations were below detection level at site 3 during the summer period (Fig. 3).

Biological mediation of Si

The key diatom taxa observed under seasonal environmental differences were *Pleurosigma*, *Gyrosigma* and *Nitzschia sigma*, similar to the findings presented by Yallop et al. (1994) following an investigation of Portishead mudflats (site 2). Chl a was significantly higher ($U_{df=176}$, $Z=-5.3102$, $p<0.001$) during cold conditions ($240 \pm 23 \text{ mg g}^{-1} \text{ sed. dw.}$) compared to warm conditions ($132 \pm 19 \text{ mg g}^{-1} \text{ sed. dw.}$), with average air temperatures having declined by 10.1°C (Fig. 2). Biofilm chl a sampled during the summer, positively correlated with BBSi (Table 3). Chl a was higher at site 3 compared

to other sampled sites in both periods of the study (Table 2). Furthermore, at site 3, under cold conditions, chl *a* positively correlated with BBSi (Table 3).

Variable chlorophyll fluorescence analysis during both warm and cold conditions was measured over periods of approximately 3 hrs, with both photoperiods subject to high irradiance levels, with peak values of 1278 $\mu\text{mol photons s}^{-1} \text{ m}^{-2}$ (summer) and 1944 $\mu\text{mol photons s}^{-1} \text{ m}^{-2}$ (winter). Diatoms exposed to warmer conditions were significantly more productive ($t(df)=5.6104$, $p<0.001$) compared to diatoms exposed to colder conditions, with $rETR_{\text{max}}$ averaging 254.1 ± 20.1 and 116.0 ± 27.1 rel. units, respectively (Table 2), thus increasing the potential for biomineralization of Si under warm conditions (Fig. 2) through enhanced rates of productivity. However, $rETR_{\text{max}}$ at site 1, sampled during the summer, negatively correlated with BBSi but positively correlated with BBSi in winter (Table 3). During cold conditions site 3, $rETR_{\text{max}}$ negatively correlated with BBSi (Table 3). Similar to $rETR_{\text{max}}$, α was higher during warmer conditions compared to cold conditions (0.22 ± 0.1 and 0.18 ± 0.02 $\mu\text{mol photons s}^{-1} \text{ m}^{-2}$, respectively).

During both warm and cold periods, a high proportion of RLCs failed to saturate, probably due to downward migration of cells away from the fluorometer light source as light intensity increased (Fig. 4). In the summer sampling period, 94% of light curves did not saturate, decreasing to 58% in the winter, suggesting a greater level of cell movement under warm conditions. F_v/F_m (0.65 ± 0.08 and 0.44 ± 0.2 rel. units) and $F_m'_{\text{max}}$ (2894 ± 614 and 1946 ± 272 rel. units) were higher under cold conditions compared to the warmer ones, respectively (Table 2). However, the high irradiance levels recorded during the winter sampling period, despite lower sunshine hours, resulted in down regulation of both α and $rETR_{\text{max}}$, which implies reduced productivity and hence reduced biomineralization of Si (Fig. 2).

As a response to high irradiance levels, the MPB biofilms performed both behavioural and physiological downregulation in order to maximise photosynthesis. Biofilms sampled during the summer were characterised by a migrational system (Fig. 4 and 5). Diatoms used downward cell movement away from increasing light levels during the RLCs, increasing F_q'/F_m' (Fig. 5). Additionally, as light levels increased there was a rise in F_m' and F' , indicating NPQ reversal alongside downward migration, causing a decrease in these fluorescence yields. As NPQ would be induced with increasing light levels, and Q_A would become reduced (both processes acting to reduce yields in the case of F'), these data (F' and F_m' yields, NPQ data, Fig. 5) suggest downward vertical

cell movement, supporting this to be the cause for the lack of saturation of RLCs (see *above*). It should be noted that, NPQ, sampled during the summer, positively correlated with BBSi (Table 3), suggesting that these migratory biofilms were sufficiently productive (higher $rETR_{max}$ and α compared to the sampled winter) to mediate BBSi, despite having lower biomass.

Biofilms sampled during the winter were characterised by high NPQ induction as a response to high irradiance, with reduced migration of the biofilms (Fig. 4 and 5), and hence a larger proportion of RLCs saturated. Residual NPQ was observed at site 2 and 3 (Fig. 5) at the beginning of the RLCs. With increasing PAR, F_m' declined, and NPQ and F' increased (Fig. 5), suggesting NPQ induction was greater, and downward cell movement was reduced, compared to the summer. A lack of downward migration was also supported by the larger decrease in F_q'/F_m' with increasing PAR increments (Fig. 5). Furthermore, NPQ_{max} sampled during the winter was higher compared to that sampled during summer (0.8 ± 0.5 and 0.19 ± 0.1 rel. units, respectively) and NPQ positively correlated with $rETR_{max}$ (Table 3).

Discussion

Microphytobenthos (MPB) biofilms under warmer summer conditions had lower biomass, and biologically mediated Si through the ecological function of the productive, high light acclimated diatoms that were highly motile during fluorescence measurements. This migratory behaviour increased the potential for growth and the formation of biofilms, which initiated the build-up of BBSi. Biofilms subject to colder winter conditions, had higher relative biomass but of low light acclimated diatoms, which had reduced migratory capabilities and induced NPQ throughout the photoperiod. Through the reduced rates of productivity the potential for biomineralization of Si may have been reduced. However, despite the high photosynthetic abilities of the diatoms, and regardless of different temperature regimes, the biological mediation of BBSi was low, with poor BDSi uptake, typical of biofilms in a dynamic intertidal estuary subject to high re-suspension and tidal influences. These dynamics resulted in low mudflat BBSi standing stocks, with estuarine Si dominated by dissolved forms, especially during cold periods with increased rainfall. In summary, environmental conditions influenced the diatom-dominated MPB biofilm biological mediation of Si, preventing sufficient accumulation of BBSi in the intertidal mudflats of the Severn Estuary. Therefore, BBSi and BDSi

concentrations were best explained by complex hydrodynamics, dissolution kinetics and terrestrial/coastal inputs rather than the biological uptake of Si.

BBSi and BDSi in the Severn Estuary

Low BBSi standing stocks in the intertidal mudflats were observed during the summer (0.6%) and winter (0.5%) sampled periods (Fig. 2). The Severn Estuary may have a low BBSi retention throughout the year (Fig. 6), similar to previous benthic Si estuarine studies (Ragueneau et al. 1994; Arndt & Regnier, 2007; Arndt et al. 2007; Jacobs, 2009; Laurelle et al. 2009; Carbonnel et al. 2009; 2013; Raimonet et al. 2013). For example, Chou & Wollast (2006) report low BBSi standing stocks in the Scheldt between 0.05% and 1.5%. Estuarine BSi and BBSi budgets are often low due to the hydro-geomorphological processes enhancing turbidity, leading to a reduction in the abundance of photosynthetic diatoms (Tréguer & De La Rocha, 2013). However, the high BDSi standing stocks (Fig. 2) suggest that the estuary can be considered as an efficient filter for DSi and may have a significant importance regarding Si cycling.

The spatial distribution of BBSi between the three sites (Fig. 6) reflected three processes; (1) settlement and biological accumulation of particulates relative to the estuarine hydrodynamics, inducing the retention of Si in more sheltered locations, (2) transportation of particulates as suspended material downstream, and (3) dissolution at biological timescales. Sediment dynamics were likely different at each sampled site. For example, the exposed mudflats at site 1 likely experienced high rates of erosion and re-suspension, which reduced BBSi standing stocks (Fig. 3), whereas the sheltered mudflats from the prevailing south westerly winds at site 3 had increased deposition, inducing the build-up of biofilms, and subsequently BBSi (Fig. 3). However, the overall low standing stocks of BBSi (Fig. 2) suggests the overall high rates of re-suspension in the estuary (Manning et al. 2010), preventing the settling and accumulation of particulates in the high water content intertidal mudflats (Table 2), coinciding with the hyper-tidal regime (Neill & Couch, 2011), were the most likely candidates to explain the observed variations in BBSi. This increased transport of BBSi to the pelagic zone may support high primary productivity in the marine zone of the Outer Bristol Channel (Morris, 1984).

The combination of high suspended particulate matter (SPM) and turbidity maxima, further explain the low mudflat BBSi concentrations. Sediment dynamics have previously been investigated for the Severn Estuary (Allen, 1990; Duquesne et al. 2006; Jonas & Millward, 2010). Manning et al. (2010) report of a turbidity maximum,

where SPM concentrations were in excess of 10 g L^{-1} in the upper estuary near site 2, which may have reduced chl *a* (Table 2) and subsequently BBSi (Fig. 3). The contribution of BBSi from the re-suspended sediments to the overall estuarine BSi budget remains unknown. Previous studies have estimated between 20% and 40% of biofilms are re-suspended (de Jonge & van Beusekom, 1992, 1995; Hanlon et al. 2006). Considering the expected high re-suspension rates and sediment loads, along with the pelagic fraction of BSi, which is expected to be small (Underwood, 2010), the overall estuarine system is unlikely to have a significant retention of BSi, despite potentially high terrestrial inputs of Si (e.g. DeMaster, 1981; Muylaert & Raine, 1999). However, a large variation in BBSi resuspension would be expected between spring and neap tides. For example, Parker & Kirby (1981) report 70% of the sediment placed into suspension on a spring tide is settled on a neap tide.

Dissolution kinetics may also explain the variations in Si between the three sampled sites (Fig. 3), where particulates were transported downstream, gradually dissolving, increasing BDSi concentrations (e.g. De'Elia et al. 1983; Yamada & De'Elia 1984). Spatial variations in nitrate, ammonium, phosphate and silicate have previously been shown in the estuary between the freshwaters end members (av. 2.7‰) to the marine end members (av. 28.3‰) (Underwood, 2010). Similarly, in the Bay of Brest (Beucher et al. 2004) and in Chesapeake Bay (De'Elia et al. 1983), BSi dissolution increased DSi retention to 48% and 65%, respectively. The Severn Estuary may exhibit similar characteristics to the Oder Estuary, including (1) higher export of Si compared to retention, (2) BBSi dissolution resulting in high BDSi retention, and (3) Si fractions dominated by dissolved forms. For example, Pastaszuak et al. (2008) suggests the Oder Estuary behaved as a source of DSi through the dissolution of ~50% of BSi into DSi, with 25% of BSi transported to a nearby Bay.

Terrestrial discharge was likely the primary environmental factor influencing the distribution and concentration of Si, and likely influenced the biofilm biological mediation of Si. For example, at the mouth of the River Severn (site 1), the highest standing stock of BDSi was recorded with concentrations averaging $24.7 \pm 1.6 \text{ mg L}^{-1}$, which correlated with high chl *a* content (Table 3). However, Morris (1984) note the River Severn only supplies a quarter of the freshwater into the estuary. Dissolution of Si may have been less significant compared to terrestrial inputs, especially during the cold winter season (Fig. 2). For example, dissolution in the Scheldt Estuary was of minor importance (3.6%) compared to the riverine influx of DSi ($5.9 \times 10^7 \text{ mol}$) (Arndt & Regnier, 2007). Terrestrial inputs likely resulted in high BDSi concentrations (Fig. 2),

especially during the winter following high rainfall in the Severn Estuary catchment area (273.5 mm; Met Office, 2015) (Fig. 2). High winter Si concentrations have previously been recorded for the estuary (Morris, 1984). In contrast, during the summer, lower rainfall (103.8 mm; Met Office, 2015) (Fig. 2) alongside peak biological activity (Table 2), likely reduced BDSi standing stocks, and led to a rise in BBSi (Fig. 2).

Terrestrial inputs may also have increased the supply of detrital BSi (BSi_{det}), e.g. phytoliths (Conley, 2002). For example, saltmarshes and wetlands have been shown (Norris & Hackney, 1999) to have significant *in situ* accumulation of phytolith BSi. BSi_{det} originating from these habitats may have been responsible for significantly ($p < 0.001$) higher BBSi concentrations (Fig. 3) and chl *a* contents (Table 2), and the significant correlations between chl *a* and $rETR_{max}$ with BBSi at site 3 (Table 3). Furthermore, BSi_{det} from the river and saltmarshes may have contributed as a source of BDSi via remineralization through pore and groundwater discharge by advective transport at high tide, and seepage at low tide (Georg et al. 2009), with phytolith dissolution proven to double DSi inputs compared to dissolution from silicate mineral weathering (Struyf et al. 2005).

Biological mediation of Si

MPB biomass and productivity

MPB biomass exhibited a significant ($p < 0.001$) difference between warmer summer conditions (13.2 mg g⁻¹ sed. dw.) and colder winter conditions (24.0 mg g⁻¹ sed. dw.) (Table 2). The low winter temperatures (Fig. 2) may have reduced diatom metabolism and/or inhibited cell movement through extracellular polymers (EPS), restricting diatoms ability to vertically migrate away from the fluorometer light source as light intensity increased, subsequently increasing the cell biomass in the surficial 5 mm.

Biomass was high compared to previous estuarine studies (e.g. Underwood & Kromkamp, 1999) and previous studies on the Severn Estuary (e.g. Underwood & Paterson, 1993; Yallop & Paterson, 1994) possibly reflecting increased cohesivity (enhanced by biostabilization), and favourable conditions necessary for benthic growth. Therefore, sites with high water content, e.g. site 2 in the sampled winter (Table 2), may have increased re-suspension rates, reducing the biofilm biomass and accumulation of BBSi (Fig. 3). However, during a tidal emersion period where sediments undergo desiccation due to de-watering, sediment of a lower water content may actually exhibit lower chl *a* content per unit weight of sediment due to an increase

in sediment bulk density, emphasising the importance to incorporate changes in water content into the calculation of chl *a* content (see Perkins et al. 2003). The change in sediment cohesivity between the summer and winter sampling periods likely influenced the variation in biofilm relative primary productivity. The biofilms sampled during the summer had high water content, and were highly productive with relative primary productivity averaging highs of 254.1 ± 20.1 rel. units, despite having lower biomass. In comparison, biofilms sampled during the colder winter period were of a lower water content, and had reduced rates of relative primary productivity (116.0 ± 27.1 rel. units), despite higher biomass (Table 2). However, the complex hydrodynamics most likely resulted in a constant turnover of the thin, unstable biofilms (Yallop et al. 1994), in line with an active transient biofilm that reduced the ecological potential to accumulate BBSi (Fig. 2). Chl *a* positively correlated with BBSi, consistent with a decline in BBSi concentrations corresponding to reduced biomass of the diatom-dominated biofilms (Table 3).

The study assumed the measured chl *a* was unique to diatoms, however it was possible that BSi_{det} and higher abundances of green algae, euglenophytes and cyanobacteria (Oppeneheim, 1998, 1991; Underwood, 1994) may have influenced chl *a* and BBSi measurements. Previous studies (Oppenheim, 1988, 1991) have shown a total of 65 taxa, with MPB composition primarily of *N. vacilla*, *Navicula viridula* var. *rostellata*, *N. humerosa* and *Diploneis littoralis*. Furthermore, diatoms having greater migratory behaviours, for example the observed *Pleurosigma*, may have reduced the surficial biomass and the biofilms rates of productivity (Cartaxana et al. 2011).

Photosynthetic ability of MPB biofilms

Biofilms subject to warmer summer conditions were significantly ($p < 0.001$) more productive and efficient compared to those subject to colder winter conditions, and exhibited strong migratory behaviour (Fig. 5). This behaviour has previously been observed in diatom-dominated biofilms (Perkins et al. 2010). MPB sampled during the summer exhibited higher α and $rETR_{max}$ (Table 2) with data (F' , F_m' yields, and NPQ, Fig. 5) suggesting downward migration was dominant, causing the lack of RLC saturation (Fig. 4). Indeed, 94% of the RLCs did not saturate. As a result of the enhanced rates of productivity there was greater biological mediation of Si and higher BBSi mudflat standing stocks in the sampled summer period (Fig. 2). A lack of RLC saturation on natural samples has previously been measured (Kromkamp et al. 1998; Perkins et al. 2002; 2010a). Comparative studies (Perkins et al. 2002; 2010b; Serôdio

et al. 2006a; 2008) have also shown migration to follow NPQ induction as diatoms acclimate to increasing light levels.

Diatoms sampled during the warmer summer period were relatively nutrient limited, with low F_v/F_m recorded at all sample sites (Table 2), correlating with BBSi (Table 3). For example, $P-PO_4^-$ was below the detection level at site 3 (Fig. 3). However, $P-PO_4^-$ negatively correlated with BBSi (Table 3), suggesting at high $P-PO_4^-$ concentrations, BDSi became limiting, potentially as a result of peak summer biological activity. Low standing stocks of BDSi have also been recorded in the Oder Estuary during peak diatom activity in the spring and summer, alongside low DSi riverine loads (which neared $0 \mu\text{mol dm}^{-3}$) (Pastuszak et al. 2008).

The significant ($p < 0.001$) difference between biofilm productivity measured during the summer and winter sampled periods was best explained by higher peak irradiance levels experienced during the winter photoperiod, resulting in downregulation (mainly in the form of NPQ induction) of both α and $rETR_{\text{max}}$ (Table 2) which led to reduced productivity and the reduced biological mediation of Si. NPQ_{max} was higher during cold conditions (0.8 ± 0.5 rel. units) compared to warmer ones (0.2 ± 0.07 rel. units) and considered in line with typical NPQ_{max} values below 4.0 rel. units (Serôdio et al. 2005). Furthermore, NPQ positively correlated with $rETR_{\text{max}}$ (Table 3), suggesting NPQ induction likely influenced winter productivity. Diatoms sampled during the colder winter period were not nutrient limited (high F_v/F_m), but were acclimated to low light and had restricted migrational activity. This contributed to the large reduction in F_q'/F_m' with increasing PAR, and resulted in a higher proportion (42%) of RLCs saturating (compared to 6% in summer), e.g. at site 2 and 3 (Fig. 4). Therefore, temperature was likely a key factor in determining the balance between behavioural and physiological down regulation of photochemistry. However, inflections in RLCs (see Perkins et al., 2001) were observed during the winter at site 2 and 3, between irradiance levels of 579-803 and 283-411 $\mu\text{mol photons s}^{-1} \text{ m}^{-2}$, respectively (Fig. 4). These S-shaped curves have occasionally been observed in *in situ* measurements of intact sediment (Perkins et al. 2002) and suggest vertical migration. Further, the large difference in PAR at which the inflections occurred may have also resulted from different diatom communities present.

Conclusions

The extensive intertidal mudflats of the hypertidal Severn Estuary are an ideal study areas to carry out a multidisciplinary analysis of Si, allowing for a comprehensive examination of estuarine internal Si cycling. Here we show environmental factors to influence the diatom-dominated biofilms ability to mediate Si. BBSi standing stocks in the mudflats were low compared to other European estuaries. Dissolved Si forms dominated the estuary, with BDSi concentrations reflecting both biological mediation with near complete consumption during the warmer summer conditions, as well as terrestrial/coastal inputs. Biofilms subject to warmer conditions biologically mediated Si by the productive, low biomass of high light acclimated diatoms that were highly motile during fluorescence measurements. This migratory behaviour, despite nutrient limitation, increased the potential for growth and the accumulation of BBSi. Biofilms subject to colder winter conditions of a higher relative biomass of low light acclimated diatoms, had reduced migratory capabilities and induced NPQ throughout the photoperiod. The potential for biomineralization of Si was scaled down as a result of lower rates of productivity under colder winter conditions. We conclude that temperature was an important driver of biofilm productivity. However, despite the high photosynthetic abilities of the diatoms, the biological mediation of BBSi was considered low during both sampled periods. BBSi and BDSi concentrations were best explained by complex hydrodynamics increasing biofilm re-suspension, dissolution kinetics and terrestrial/coastal inputs rather than the biological uptake of Si. However, the estuaries importance for Si cycling on a wider geographical scale, considering the high BDSi standing stocks, high rates of re-suspended BBSi and all external inputs of Si, requires further work into, 1) the benthic-pelagic coupling, 2) transportation of Si and nutrients along the tidal river, estuary and coastal zone, and 3) the influence of the complex tidal regime and sediment dynamics (through re-suspension and mineralization) on Si over spatial and temporal scales.

Acknowledgments

The project was developed as part of an Integrated Masters in Marine Geoscience at Cardiff University School of Earth and Ocean Science. We acknowledge the role of J. Pinnion (Cardiff University) and G. Wallington for their fieldwork assistance, and L. Axe (Cardiff University) who assisted with the SEM analysis. We would also like to thank Natural Resource Wales and Newport Wetland Reserve for their assistance in the project. We thank the two anonymous reviewers for their constructive comments and help in improving the manuscript.

References

- Allen, J. 1990. The Severn Estuary in southwest Britain: its retreat under marine transgression, and fine-sediment regime. *Sedimentary Geology*. 66:13–28.
- Arndt, S., Regnier, P. 2007. A model for the benthic-pelagic coupling of silica in estuarine ecosystems: sensitivity analysis and system scale simulation. *Biogeosciences*. 4:331–352.
- Arndt, S., Vanderborght, J., Regnier, P. 2007. Diatom growth response to physical forcing in a macrotidal estuary: Coupling hydrodynamics, sediment transport, and biogeochemistry. *J. Geophys. Res.* 112.
- Aure, J., Danielssen, D., Svendsen, E. 1998. The origin of Skagerrak coastal water off Arendal in relation to variations in nutrient concentrations. *ICES J. Mar. Sci.* 55:610 – 619.
- Beucher, C., Tréguer, P., Corvaisier, R., Hapette, A., Elskens, M. 2004. Production and dissolution of biosilica, and changing microphytoplankton dominance in the Bay of Brest (France). *Mar Ecol Prog Ser.* 267:57–69.
- Brzezinski, M., Villareal, T., Lipschultz, F. 1998. Silica production and the contribution of diatoms to new and primary production in the Central North Pacific. *Mar. Ecol.: Prog. Ser.* 167:89–104.
- Carbonnel, V., Lionard, L., Muylaert, K., Chou, L. 2009. Dynamics of dissolved and biogenic silica in the freshwater reaches of a macrotidal estuary (The Scheldt, Belgium). *Biogeochemistry*. 96:49–72.
- Carbonnel, V., Vanderborght, J., Chou, L. 2013. Silica Mass-Balance and Retention in the Riverine and Estuarine Scheldt Tidal System (Belgium/The Netherlands). *Aquatic Geochemistry*. 19:501–516.
- Cartaxana, P., Ruivo, M., Hubas, C., Davidson, I., Serôdio, J., Jesus, B. 2011. Physiological verses behavioural photoprotection in intertidal epipellic and epipsamic benthic diatom communities. *Journal of Experimental Marine Biology Ecology*. 405:120–127.
- Conley, D., Malone, T. 1992. Annual cycle of dissolved silicate in Chesapeake Bay: implications for the production and fate of phytoplankton biomass. *Marine Ecology Progress Series*. 81:121–128.
- Conley, D. 2002. Terrestrial ecosystems and the global biogeochemical silica cycle. *Global Biogeochemical Cycles*. 16(4):68–75.
- Correll, D., Jordan, T., Weller, D. 2000. Dissolved silicate dynamics of the Rhode river watershed and estuary. *Estuaries*. 23:188–198.
- Chou, L., Wollast, R. 2006. Estuarine silicon dynamics, in: *The Silicon Cycle: Human Perturbations and Impacts on Aquatic Systems*, edited by: Ittekkot, D., Unger, C., Humborg, C., and Tac An. Island Press, Washington, Covelo, London. 66:93–120.
- DeMaster, D. 1981. The supply and accumulation of silica in the marine environment. *Geochimica et Cosmochimica Acta*. 45:1715–1732.
- De'Elia, C., Nelson, D., Bonton, W. 1983. Chesapeake Bay nutrient and plankton dynamics: III. The annual cycle of dissolved silicon. *Geochim Cosmochim Acta*. 47:1945–1955.
- de Jonge, V., van Beusekom, J. 1992. Contributions of re-suspended microphytobenthos to total phytoplankton in the Ems estuary and its possible role for grazers. *Netherlands Journal of Sea Research*. 30:91–105.
- de Jonge, V., van Beusekom, J. 1995. Wind- and tide-induced resuspension of sediment microphytobenthos from the tidal flats in the Ems estuary. *Limnology and Oceanography*. 40:766–778.
- Duquesne, S., Newton, L., Giusti, L., Marriott, S., Stark, H., Bird, D. 2006. Evidence for declining levels of heavy-metals in the Severn Estuary and Bristol Channel, UK and their spatial distribution in sediments. *Environmental Pollution*. 143:187–196.

- Eilers, P., Peeters, J. 1988. A model for the relationship between light intensity and the rate of photosynthesis in phytoplankton. *Ecological Modelling*. 42:199-215.
- Fortner, S., Lyons, W., Carey, A., Shipitalo, M., Welch, S., Welch, K. 2012. Silicate weathering and CO₂ consumption within agricultural landscapes, the Ohio-Tennessee River Basin, USA S. K. *Biogeosciences*. 9:941-955.
- Genty, B., Briantais, J., Baker, N. 1989. The relationship between the quantum yield of photosynthetic electron transport and quenching of chlorophyll fluorescence. *Biochimica et Biophysica Acta*. 990:87-92.
- Georg, R., West, A., Basu, A., Halliday, A. 2009. Silicon fluxes and isotope composition of direct groundwater discharge into the Bay of Bengal and the effect on the global ocean silicon isotope budget. *Earth and Planetary Science Letters*. 283:67-74.
- Gilpin, L., Davidson, K., Roberts, E. 2004. The influence of changes in nitrogen: silicon ratios on diatom growth dynamics. *Journal of Sea Research*. 51:21-35.
- Hammer, O., Harper, D., Ryan, P. 2001. PAST: Paleontological statistics software package for education and data analysis. [online] Available in: <http://palaeo-electronica.org/2001_1/past/issue1_01.htm>.
- Hanlon, A., Bellinger, B., Haynes, K., Xiao, G., Hofmann, T., Gretz, M., Ball, A., Osborn, A., Underwood, G. 2006. Dynamics of extracellular polymeric substance (EPS) production and loss in an estuarine, diatom-dominated, microalgal biofilm over a tidal emersion-immersion period. *Limnology and Oceanography*. 21:79-93.
- Hurd, D. 1977. The effects of glacial weathering on silica budget of Antarctica waters. *Geochim Cosmochim Acta*. 41:1213-1222.
- Jacobs, S. 2009. Silica cycling and vegetation development in a restored freshwater tidal marsh. 1-198.
- Jesus, B., Perkins, R., Consalvey, M., Brotas, V., Paterson, D. 2006. Effects of vertical migrations by benthic microalgae on fluorescence measurements of photophysiology. *Marine Ecology Progress Series*. 315:55-66.
- Jonas, P., Millward, G. 2010. Metals and nutrients in the Severn Estuary and Bristol Channel: contemporary inputs and distributions. *Marine Pollution Bulletin*. 61(1-3):52-67.
- Kromkamp, J., Barranguet, C., Peene, J. 1998. Determination of microphytobenthos PSII quantum efficiency and photosynthetic activity by means of variable chlorophyll fluorescence. *Marine Ecology Progress Series*. 62:45-55.
- Kirby, 2010. Distribution, transport and exchanges of fine sediment, with tidal power implications: Severn Estuary, UK. *Marine Pollution Bulletin*. 61:21-36.
- Lavaud, J., Kroth, P. 2006. In diatoms, the transthylakoid proton gradient regulates the photoprotective non-photochemical fluorescence quenching beyond its control on the xanthophyll cycle. *Plant Cell Physiology*. 47:1010-1016.
- Lavaud, J. 2007. Fast regulation of photosynthesis in diatoms: mechanisms, evolution and ecophysiology. *Plant Science and Biotechnology*. 1:267-287.
- Liang, D., Junqiang, X., Falconer, R., Zhang, J. 2013. Study on Tidal Resonance in Severn Estuary and Bristol Channel. *Coastal Engineering Journal*. 56(1):1-18.
- Liu, W., Hsu, M., Chen, S., Wu, C., Kuo, A. 2005. Water column light attenuation Danshuei river estuary, Taiwan. *Journal of the American Water Resource Association*. 425-435.
- Liu, S., Ye, X., Zhang, L., Zhang, G., Wu, Y. 2008. The silicon balance in Jiaozhou Bay, North China. *J Mar Syst*. 74:639-648.
- Liu, S., Hong, G., Zhang, J., Ye, X., Jiang, X. 2009. Nutrient budget of large Chinese estuaries. *Biogeosciences*. 6:2245-2263.
- Lorenzen, C. 1966. A method for the continuous measurement of in vivo chlorophyll concentration. *Deep-Sea Research*. 13: 223-227.
- Manning, A., Langston, W., Jonas, P. 2010. A review of sediment dynamics in the Severn Estuary: Influence of flocculation. *Marine Pollution Bulletin*. 61:37-51.

- Maxwell, K., Johnson, G. 2000. Chlorophyll fluorescence-a practical guide. *Journal of Experimental Botany*. 51:659–668.
- Met Office. 2011. Climate: Observations, projections and impacts. [pdf] Met Office. Available in: <<http://www.metoffice.gov.uk/media/pdf/t/r/UK.pdf>> [Accessed 2015].
- Met Office. 2015. UK climate: download regional values. [pdf] Met Office. Available in: <<http://www.metoffice.gov.uk/climate/uk/summaries/datasets>> [Accessed 2015].
- Moosdorf, N., Hartmann, J., Lauerwald, R. 2011. Changes in dissolved silica mobilization into river systems draining North America until the period 2081–2100. *Journal of Geochemical Exploration*. 110(1):31-39.
- Morris, R. 1984. The chemistry of the Severn Estuary and the Bristol Channel. *Marine Pollution Bulletin*. 15(2):57-61.
- Muylaert, K., Raine, R. 1999. Import, mortality and accumulation of coastal phytoplankton in a partially mixed estuary (Kinsale harbour, Ireland). *Hydrobiologia*. 412:53-65.
- Norris, A., Hackney, C. 1999. Silica content of a mesohaline tidal marsh in North Carolina. *Estuarine Coastal Shelf Science*. 49:597-605.
- Neill, S., Couch, S. 2011. Impact of Tidal Energy Converter (TEC) array operation on sediment dynamics. *Renewable Energy*. 37:387-397.
- Oppenheim, D. 1988. The distribution of epipellic diatoms along an intertidal shore in relation to principal physical gradients. *Botanica Marina*. 31:65–72.
- Oppenheim, D. 1991. Seasonal changes in epipellic diatoms along an intertidal shore, Berrow flats, Somerset. *Journal of the Marine Biological Association of the United Kingdom*. 71:579–596.
- Parker, W., Kirby, R. 1981. The behaviour of cohesive sediment in the inner Bristol Channel and Severn Estuary in relation to construction of the Severn Barrage (Unpublished). *Institute of oceanographic sciences*. 117: 1-39.
- Pastuszek, M., Conley, D., Humborg, C., Witek, Z., Sitek, S. 2008. Silicon dynamics in the Oder estuary, Baltic Sea. *Journal Marine System*. 73:250-262.
- Perkins, R., Underwood, G., Brotas, V., Snow, G., Jesus, B., Ribeiro, L. 2001. Responses of microphytobenthos to light: primary production and carbohydrate allocation over an emersion period. *Marine Ecology Progress Series*. 223:101–12.
- Perkins, R., Oxborough, K., Hanlon, A., Underwood, G., Baker, N. 2002. Can chlorophyll fluorescence be used to estimate the rate of photosynthetic electron transport within microphytobenthic biofilms? *Marine Ecology Progress Series*. 228:47–56.
- Perkins, R., Honeywill, C., Consalvey, M., Paterson, D. 2003. Changes in microphytobenthic chlorophyll *a* and EPS resulting from sediment compaction due to de-watering: opposing patterns in concentration and content. *Continental shelf science*. 23(6):575-586.
- Perkins, R., Mouget, J., Lefevre, S. 2006. Light response curve methodology and possible implications in the application of chlorophyll fluorescence to benthic diatoms. *Marine Biology*. 149:703-712.
- Perkins, R., Lavaud, J., Mouget, S., Cartaxana, P., Rosa, P., Barille, L., Brotas, V., Jesus, B. 2010a. Vertical cell movement is a primary response of intertidal benthic biofilms to increasing light dose. *Marine Ecology Progress Series*. 416:93-103.
- Perkins, R., Kromkamp, J., Serôdio, J., Lavaud, J., Jesus, B., Mouget, J., Lefebvre, S., Forster, R. 2010b. The application of variable chlorophyll fluorescence to microphytobenthic biofilms. In: Suggett, D., Borowitzka, M., Prášil, O. eds. *Chlorophyll *a* Fluorescence in Aquatic Sciences: Methods and Applications*. Developments in Applied Phycology. London: Springer. 4:237-275.

- Pickney, J., Zingmark, R. 1991. Effects of tidal stage and sun angles on intertidal benthic microalgae productivity. *Marine Ecology progress Series*. 76:81-89.
- Raimonet, M., Andrieux, L., Ragueneau, O., Michaus, E., Kerouel, R., Philippon, X., Nonent, M., Laurent, M. 2013. Strong gradient of benthic biogeochemical processes along a macrotidal temperate estuary: focus on P and Si cycles. *Biogeochemistry*. 115:399-417.
- Ragueneau O, De Blas Varela E, Tréguer P, Quéguiner B, Del Amo Y. 1994. Phytoplankton dynamics in relation to the biogeochemical cycle of silicon in a coastal ecosystem of western Europe. *Mar Ecol Prog Ser*. 106:157–172.
- Ragueneau, O., Tréguer, P., Leynaert, A., Anderson, R., Brzezinski, M., DeMaster, D., Dugdale, R., Dymond, J., Fischer, G., Francois, R., Heinze, C., Maier-Reimer, E., Martin-Jézéquel, V., Nelson, D., Quéguiner, B. 2000. A review of the Si cycle in the modern oceans: recent progress and missing gaps in the application of biogenic opal as a paleoproductivity proxy. *Global Planet Change*. 26(4): 317-365.
- Redfield, A., Ketchum, B., Richards, F. 1963. The influence of organisms on the composition of sea water in the sea. 2:26-77.
- Rendell, A, Horrobin, T., Jickells, T., Edmunds, H., Brown, J., Malcom, S. 1997. Nutrient cycling in the Great Ouse estuary and its impact on nutrient fluxes to The Wash, England. *Estuar Coast Shelf Sci*. 45(5):653-668.
- Serôdio, J., Cruz, S., Vieira, S., Brotas, V. 2005. Non-photochemical quenching of chlorophyll fluorescence and operation of the xanthophyll cycle in estuarine microphytobenthos. *Journal of Experimental Marine Biology Ecology*. 326:157-169.
- Serôdio, J., Vieira, S., Cruz, S., Coelho, H. 2006a. Rapid light response curves of chlorophyll fluorescence in microalgae: relationship to steady-state light curves and non-photochemical quenching in benthic diatom-dominated assemblages. *Photosynthesis Research*. 90:29–43.
- Serôdio, J., Coelho, H., Vieira, S., Cruz, S. 2006b. Microphytobenthos vertical migratory photoresponse as characterised by light-response curves of surface biomass. *Estuarine Coastal and Shelf Science*. 68:547-556.
- Serôdio, J., Vieira, S., Cruz, S. 2008. Photosynthetic activity, photoprotection and photoinhibition in intertidal microphytobenthos as studied in situ using variable chlorophyll fluorescence. *Continental Shelf Research*. 28:1363-1375.
- Shwartz, S., Lorenzo, T. 1990. Chlorophyll in foods. *Food Science and Nutrition*. 29(1):1-17.
- Smith, D., Underwood, G. 1998. Exopolymer production by intertidal epipellic diatoms. *Limnol. Oceanogr*. 43(7): 1578-1591.
- Struyf, E., Damme, S., Gribsholt, B., Meir, P. 2005. Freshwater marshes as dissolved silica recyclers in an estuarine environment (Schelde estuary, Belgium). *Hydrobiologia*. 540:69–77.
- Teasdale, P., Batley, G., Apte, S., Webster, I. 1995. Pore water sampling with sediment peepers. *Trends Anal. Chem*. 14:250–256.
- Tréguer, P., De La Rocha, C. 2013. The World Ocean Silica Cycle. *Marine Science*. 5(5.1):2-25.
- Underwood, G. 1994. Seasonal and spatial variation in epipellic diatom assemblages in the Severn Estuary. *Diatom Research*. 9:451-472.
- Underwood, G., Kromkamp, J. 1999. Primary production by phytoplankton and microphytobenthos in estuaries. *Advance in Ecology Press*. 29:93–153.
- Underwood, G. 2010. Microphytobenthos and phytoplankton in the Severn Estuary, UK: Present situation and possible consequences of a tidal energy barrage. *Marine Pollution Bulletin*. 61:83–91.
- Underwood, G., Paterson, D. 1993. Recovery of intertidal benthic diatoms from biocide treatment and associated sediment dynamics. *Journal of the Marine Biological Association of the United Kingdom*. 73:25–45.

- West, A., Galy, A., Bickle, M. 2005. Tectonic and climatic controls on silicate weathering. *Earth and Planetary Science Letters*. 235:211–228.
- Yamada, S., De'Elia, C. 1984. Silicic acid regeneration from estuarine sediment cores. *Marine Ecology Progress Series*. 18:113-118.
- Yallop, M., Winder, B., Paterson, D., Stal, L. 1994. Comparative structure, primary production and biogenic stabilization of cohesive and non-cohesive marine sediments inhabited by microphytobenthos. *Estuarine, Coastal and Shelf Science*. 39(6):565-582.
- Yallop, M., Paterson, D. 1994. Survey of Severn estuary. In: Krumbein, W., Paterson, D., Stal, L.(Eds.), *Biostabilization of Sediments*. Bibliotheks und Informationssystem der Universität Oldenburg (BIS). Verlag, Oldenburg, pp. 279–326.

Figure Captions

Figure 1. Severn Estuary intertidal mudflat study area. Severn Estuary (A) is situated in the southwest of UK (B). Tidal limit in the River Severn reaches Maisemore, north Gloucester. Outer Severn Estuary limit identified as a transect between Lavernock Point and Sand Point (14 km wide), near Weston-Super-Mare. Mudflats north of Severn Bridge are sandy, whilst lateral banks south of the bridge are predominantly muddy. Estuary discharges into Bristol Channel followed by the Irish Sea and the North Atlantic Ocean. Bathymetry of the Severn Estuary (C). DTM of the coastline around the Severn Estuary (D).

Figure. 2. Standing stocks of BDSi (A) and BBSi (B) in the Severn Estuary intertidal mudflats. Rainfall (mm) for the Severn Estuary catchment area and average air temperature (°C) for the summer and winter sampled months (Met Office, 2015). Error bars are the standard error in the calculation of the average BDSi and BBSi concentration, rainfall and temperature. BBSi: benthic biogenic silica, $n=36$ (summer), $n=35$ (winter). BDSi: benthic dissolved silicon, $n=36$ (summer), $n=36$ (winter).

Figure. 3. Distribution of BDSi and BBSi during the summer (A) and winter (B), and P- PO_4^- concentration (C) in the Severn Estuary from the upper estuary (Severn Beach, site 1), to the mid-estuary (Portishead, site 2) and the lower mid-estuary (Newport Wetlands, site 3). Error bars are the standard error in the calculation of the average BDSi, BBSi and P- PO_4^- concentration. BBSi: benthic biogenic silica, $n=36$ (summer), $n=35$ (winter). BDSi: benthic dissolved silicon, $n=36$ (summer), $n=36$ (winter). P- PO_4^- : orthophosphate, $n=36$ (summer), $n=36$ (winter).

Figure. 4. Rapid Light Curves for the summer (A) and winter (B). Downregulation interference (S-shaped) curves in winter RLCs at site 3 (light grey) and site 2 (dark grey).

Figure. 5. Diatom photosynthetic activity and downregulation processes. A-C) Summer chlorophyll fluorescence. D-F) Winter chlorophyll fluorescence. A and D) Site 1: $n=11$, $n=10$. B and E) Site 2: $n=11$, $n=5$. C and F) Site 3: $n=11$, $n=3$. Chlorophyll fluorescence (F' and F_m'). F' : minimum fluorescence yield in actinic light. F_m' : maximum fluorescence yield in actinic light. PSII efficiency (F_q'/F_m'): maximum photosynthetic efficiency of PSII. NPQ: non-photochemical quenching. PAR: photosynthetically available radiation.

Figure. 6. BBSi and BDSi dynamics in the Severn Estuary in the summer (A) and winter (B). Cylinders represent biofilm biomass. Dark arrows represent river sources. Arrows represent export of BBSi (light grey) and BDSi (black) to the coastal zone. BBSi: benthic biogenic silica. BDSi: benthic dissolved silicon.

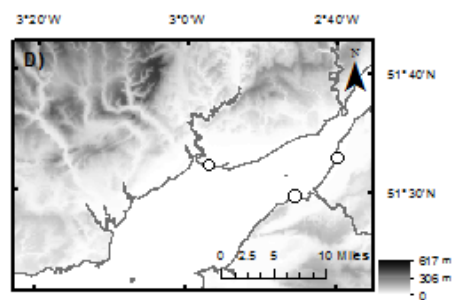
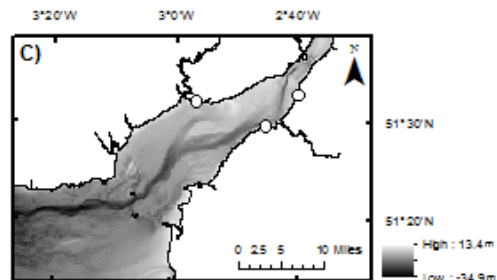
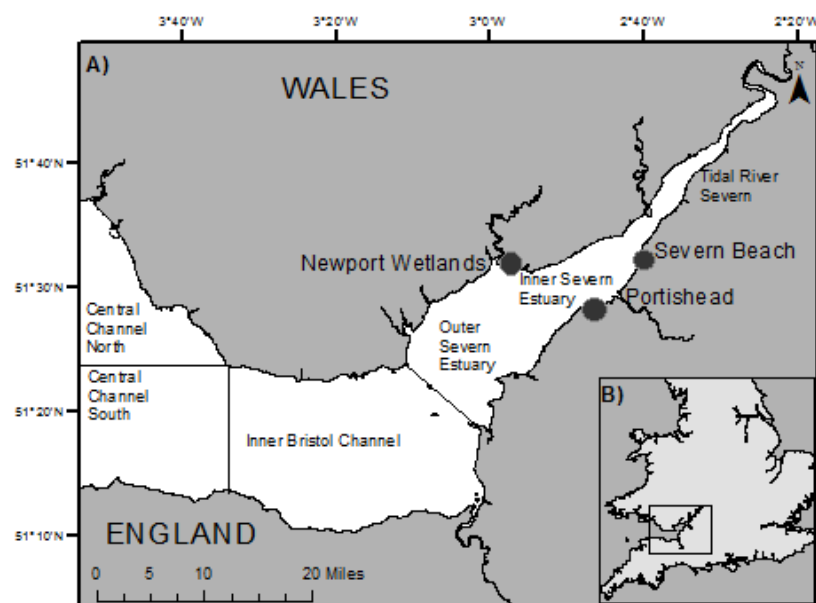
Table Captions

Table 1. Notations for silicon parameters, nutrients, biomass and chlorophyll fluorescence.

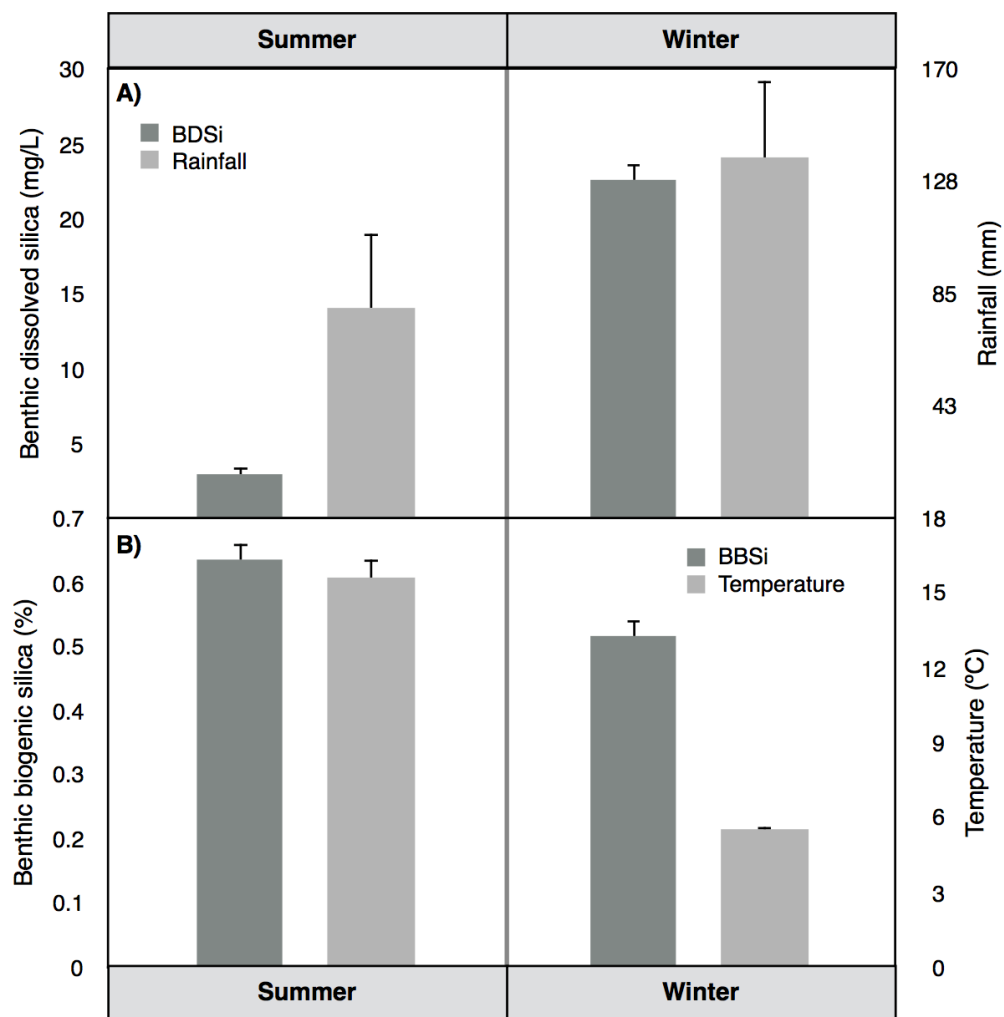
Table 2. Microphytobenthos biomass and variable chlorophyll fluorescence parameters. Values reported with standard deviation \pm SD. Chl *a*: chlorophyll *a*: $n=36$ (summer), $n=36$ (winter). $rETR_{max}$: relative maximum Electron Transport Rate: $n=34$ (summer), $n=18$ (winter). α : maximum light use coefficient: $n=34$ (summer), $n=18$ (winter). F_v/F_m : ecological health, $n=34$ (summer), $n=27$ (winter). NPQ_{max} : maximum non-photochemical quenching, $n=34$ (summer), $n=17$ (winter). F_m' : maximum PSII Chl fluorescence yield in actinic light when all reaction centres are closed: $n=34$ (summer), $n=27$ (winter). $F_{m'm}$: maximum F_m' value under low actinic light, $n=34$ (summer), $n=17$ (winter).

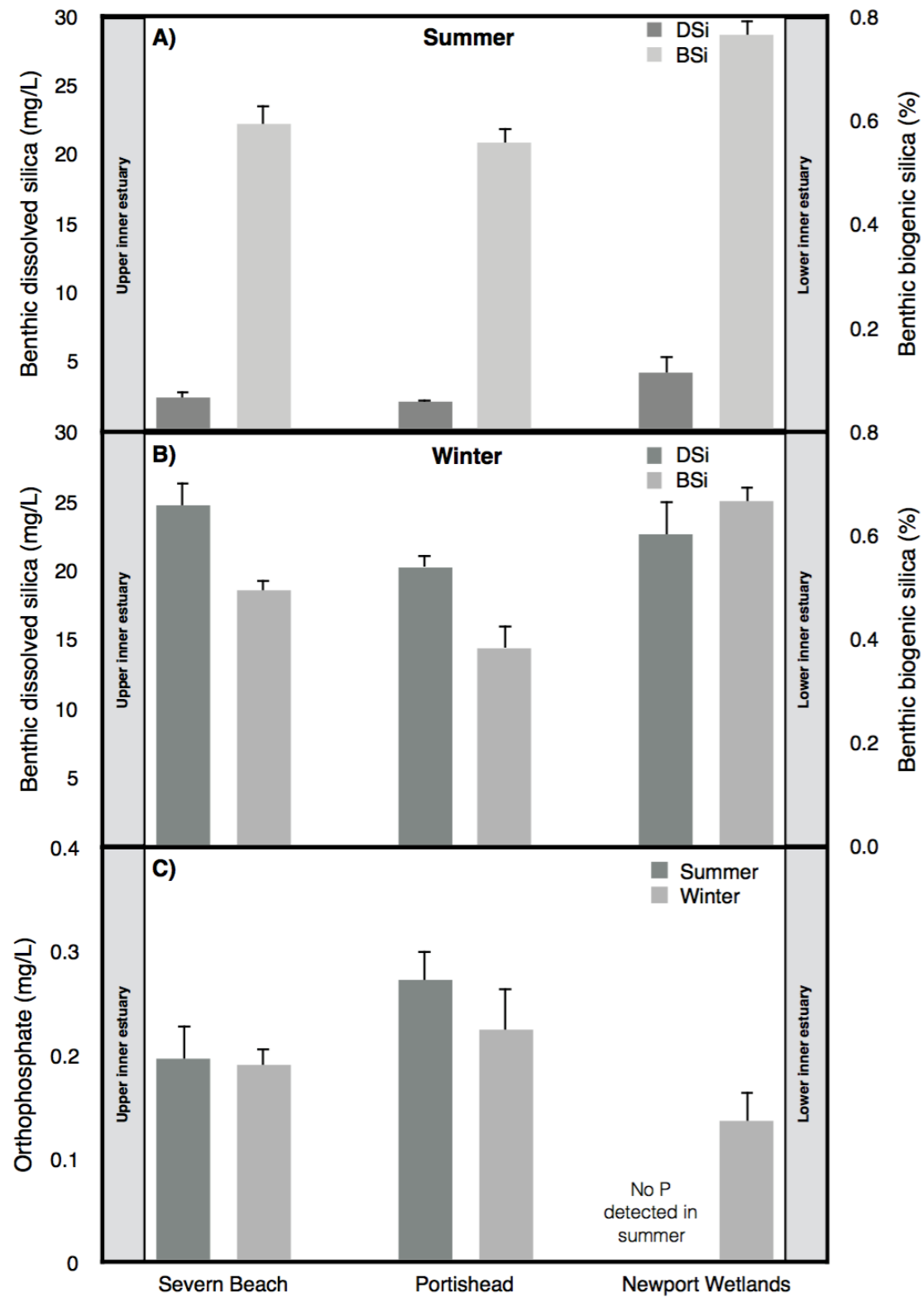
Table 3. Key drivers of BBSi and BDSi during the summer and winter in the Severn Estuary. Pearson's correlations reported with coefficient values (r) and number of samples (n). Significant correlations ($p<0.05$) are shown in **bold**. BBSi: benthic biogenic silica. BDSi: benthic dissolved silicon. Chl *a*: chlorophyll *a*. $rETR_{max}$: relative

maximum Electron Transport Rate. α : maximum light use coefficient. F_v/F_m : ecological health. NPQ: non-photochemical quenching.

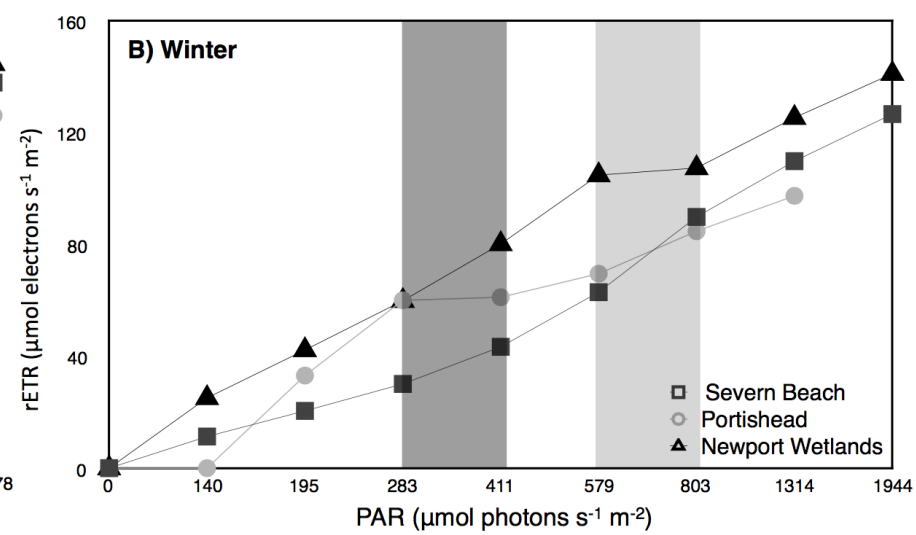
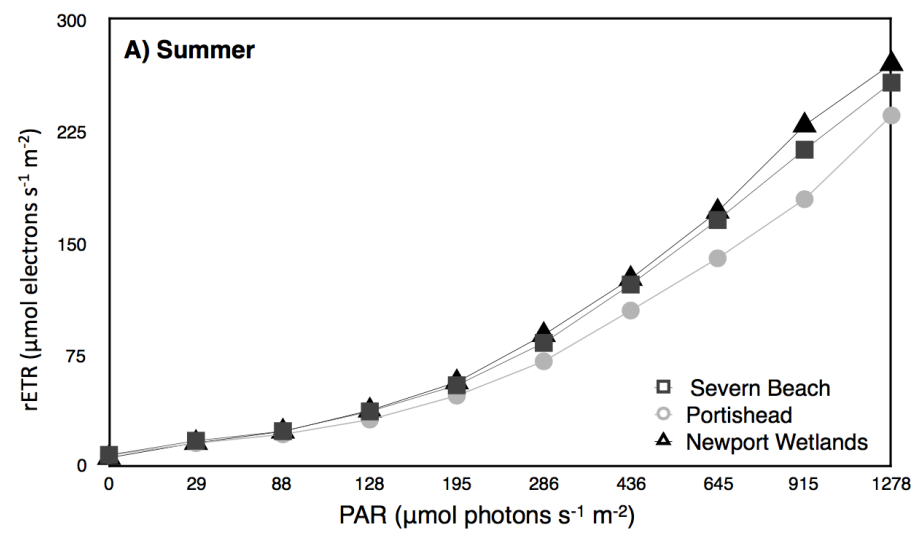


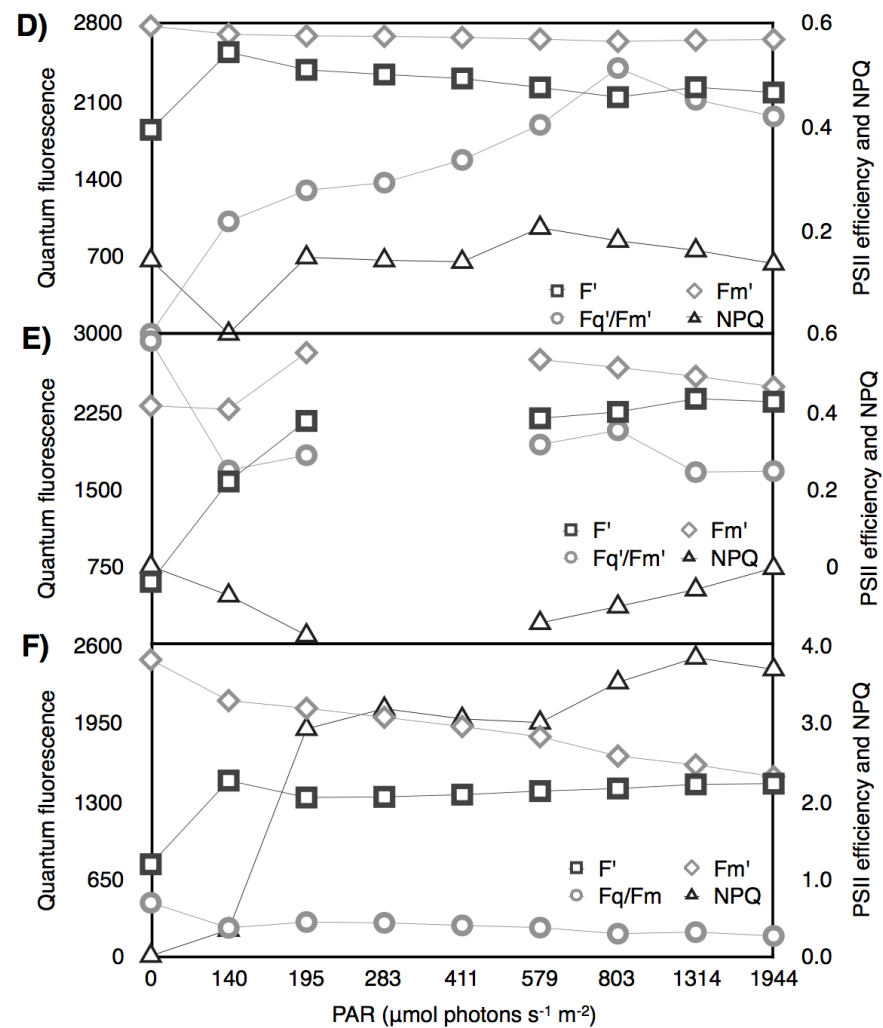
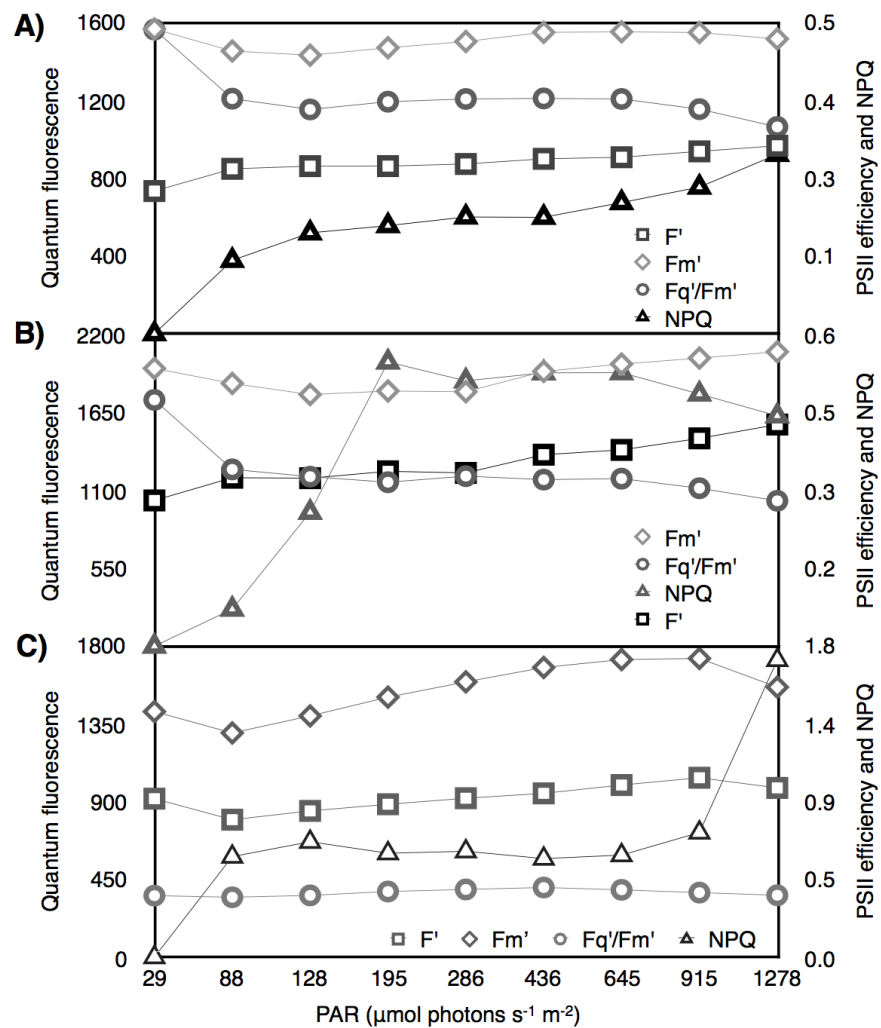
Parameter	Description
BSi	Biogenic silica
BBSi	Benthic biogenic silica
DSi	Dissolved silica
BDSi	Benthic dissolved silica
P	Orthophosphate
MPB	Microphytobenthos
Chl <i>a</i>	Chlorophyll <i>a</i> (proxy for biomass)
F'	Operational PSII Chl fluorescence yield in actinic light
F_m'	Maximum PSII Chl fluorescence yield in actinic light when all reaction centres are closed
$F_{m' \max}$	Maximum F_m'
RLC	Rapid Light Curve
PAR	Photosynthetically available radiation
$rETR_{\max}$	Relative Maximum Electron Transport Rate
α	Maximum light use coefficient for PSII
F_q'/F_m'	Maximum quantum efficiency of PSII
F_v/F_m	Maximum photochemical yield (MPB biofilm health)
NPQ	Non-photochemical quenching
NPQ_{\max}	Maximum non-photochemical quenching





Location	Site	Chl <i>a</i> (mg g ⁻¹ sed. dw.)	Water content (%)	rETR _{max} (rel. units)	α (μmol photons m ⁻² s ⁻¹)	F _v /F _m (rel. units)	NPQ _{max} (rel. units)	F _m ⁺ max (rel. units)
<i>Summer</i>								
Severn Beach	1	11.0 ± 1.9	54.9 ± 0.4	257.2 ± 16.9	0.24 ± 0.02	0.48 ± 0.5	0.3 ± 0.03	1713 ± 180
Portishead	2	11.3 ± 2.1	51.8 ± 0.8	235.2 ± 27.6	0.23 ± 0.02	0.47 ± 0.0	0.12 ± 0.1	2314 ± 320
Newport Wetlands	3	17.3 ± 1.7	65.2 ± 0.6	269.8 ± 15.9	0.18 ± 0.03	0.36 ± 0.1	0.11 ± 0.1	1813 ± 332
Average		13.2 ± 1.9	57.3 ± 0.6	254.1 ± 20.1	0.2 ± 0.02	0.44 ± 0.2	0.17 ± 0.1	1946 ± 277
<i>Winter</i>								
Severn Beach	1	24.5 ± 2.6	53.2 ± 0.8	109.7 ± 21.5	0.10 ± 0.1	0.65 ± 0.1	0.17 ± 0.0	2765 ± 798
Portishead	2	21.3 ± 1.6	57.9 ± 0.8	97.3 ± 20.8	0.17 ± 0.04	0.63 ± 0.1	0.18 ± 0.0	3318 ± 637
Newport Wetlands	3	26.0 ± 2.8	53.8 ± 0.9	141.0 ± 39.1	0.20 ± 0.01	0.67 ± 0.0	1.3 ± 0.78	2601 ± 408
Average		24.0 ± 2.3	55.0 ± 0.8	116.0 ± 27.1	0.16 ± 0.05	0.65 ± 0.1	0.84 ± 0.4	2894 ± 614





		Summer								Winter							
		Site 1		Site 2		Site 3		All		Site 1		Site 2		Site 3		All	
		<i>n</i>	<i>r</i>	<i>n</i>	<i>r</i>	<i>n</i>	<i>r</i>	<i>n</i>	<i>r</i>	<i>n</i>	<i>r</i>	<i>n</i>	<i>r</i>	<i>n</i>	<i>r</i>	<i>n</i>	<i>r</i>
BBSi drivers																	
BDSi vs. BBSi	12	0.017	12	-0.242	12	-0.349	36	0.105		12	0.105	12	-0.048	12	0.271	36	0.168
P vs. BBSi	12	0.120	12	0.413	12	-	36	-0.434		12	-0.269	12	0.163	12	-0.256	36	0.223
Chl <i>a</i> vs. BBSi	12	-0.010	12	-0.049	12	0.226	36	0.296		12	0.411	12	-0.607	12	0.541	36	-0.264
rETR _{max} vs. BBSi	11	-0.679	11	0.001	12	-0.471	34	-0.136		3	0.877	5	-0.410	10	-0.617	18	-0.058
α vs. BBSi	11	-0.259	11	0.380	12	-0.220	34	-0.289		3	-0.185	5	0.604	10	-0.411	18	0.203
F _v /F _m vs. BBSi	11	-0.326	11	0.382	12	-0.224	35	-0.291		10	-0.058	5	-0.292	12	0.038	32	-0.001
NPQ vs. BBSi	11	0.552	11	0.127	12	0.761	34	0.289		3	-0.115	4	0.557	10	-0.0	17	0.226
BDSi drivers																	
P vs. BDSi	12	0.160	12	0.444	12	-	36	-0.248		12	0.358	12	0.325	12	-0.485	36	-0.115
Chl <i>a</i> vs. BDSi	12	0.498	12	0.309	12	-0.239	36	0.160		12	-0.480	12	0.313	12	0.100	36	-0.022
rETR _{max} vs. BDSi	11	0.132	11	-0.247	12	-0.018	34	0.069		3	-0.151	5	-0.011	10	-0.026	18	0.010
α vs. BDSi	11	-0.244	11	0.380	12	0.033	34	-0.160		3	-0.987	5	0.093	10	0.207	18	-0.040
F _v /F _m vs. BDSi	11	-0.215	11	-0.409	12	0.061	35	-0.135		10	0.205	5	-0.211	12	0.209	32	0.147
NPQ vs. BDSi	11	0.018	11	0.044	12	-0.082	34	-0.053		3	-0.972	4	0.193	10	-0.328	17	-0.286

